Supporting Information

Synergistic Enhancement of Charge Extraction and Heat Dissipation in Inverted Perovskite Solar Cells via n-Doped Top Interlayers

Sangmi Park, †[a] Sang Young Jeong, †[b] Jaehoon Kim, †[c] Heunjeong Lee, [d] Hye Seung Kim, [a] Young Wook Noh, [a] Ye In Kim, [a] Shinuk Cho, [d] Joon Sang Kang, *[c] Han Young Woo *[b] and Myoung Hoon Song *[a]

[a] S. Park, H. S. Kim, Y. W. Noh, Y. I. Kim, Prof. M. H. Song
Department of Materials Science and Engineering, Ulsan National Institute of Science and Technology (UNIST), UNIST-gil 50, Ulsan 44919, Republic of Korea.
*E-mail: mhsong@unist.ac.kr

[b] S. Y. Jeong, Prof. H. Y. Woo
Department of Chemistry, Korea University, Seoul 02841, Republic of Korea.
*E-mail: hywoo@korea.ac.kr

[c] J. Kim, Prof. J. S. Kang
Department of Mechanical Engineering, Korea Advanced Institute of Science and Technology (KAIST), Daejeon 34120, Republic of Korea.
*E-mail: jskang1@kaist.ac.kr

[d] H. Lee, Prof. S. Cho
Department of Physics and EHSRC, University of Ulsan, Ulsan 44610, Republic of Korea.

Keywords: perovskite solar cells, interlayer, n-doping, stability, heat dissipation

Experimental Section

Materials

All chemicals utilized in the synthesis and device fabrication were purchased from Sigma-Aldrich, Tokyo Chemical Industry, and Alfa Aesar, and used without additional purification unless otherwise specified. [4-(3,6-Dimethoxy-9H-carbazol-9-yl)ethyl]phosphonic acid (MeO-4PACz, TCI), formamidinium iodide (FAI, Greatcell Solar), lead iodide (PbI_2, TCI), cesium iodide (CsI, ultra-dry, 99.999% (metal basis), Alfa Aesar), fullerene (C_{60}, 99.99%, OSM), and silver (Ag, 1-4 mm shot, 99.9999%, iTASCO).

Synthesis

[6,6]-Phenyl-C_{61}-butyric acid 2-[2-(2-methoxyethoxy)ethoxy]ethyl ester ($PC_{61}B$-TEG) was synthesized by following the previously reported procedures.[1-2]

^{1}H NMR (500 MHz, $CDCl_3$): δ (ppm) 7.94-7.82 (m, 2H), 7.56-7.53 (m, 2H), 7.49-7.46 (m, 1H), 4.25-4.23 (m, 2H), 3.70-3.63 (m, 8H), 3.56-3.54 (m, 2H), 3.38 (s, 3H), 2.93-2.89 (m, 2H), 2.55 (t, 2H, J = 7.50 Hz), 2.22-2.19 (m, 2H).

Instruments and Characterization

The ^{1}H NMR spectra were acquired using a Bruker Avance III HD 500 spectrometer. SEM images were captured using SU8220 Cold FE-SEM and SU7000 FE-SEM. AFM images were obtained using Dimension ICON (Bruker Nano Surface). XRD patterns were obtained using an X-ray diffractometer (D/MAX2500C/PC, Rigaku) with a Cu-rotating anode X-ray. The *J-V* characteristics of the PeSCs were measured using an Ivium-n-Stat source meter under AM 1.5 G (100 mW cm^{-2}) conditions. The EQE spectra were obtained using a QE measurement system (HS Technologies) by employing monochromatic light from a Xe lamp under ambient conditions. TPV and TPC measurements were carried out with a McScience T4000 (organic semiconductor parameter test system) at V_{OC} under illumination. XPS spectra were obtained by an Escalab 250Xi instrument (Thermo Fisher Co.), utilizing an Al Kα monochromatic X-ray

source. Casa XPS software was employed for data analysis. UPS spectra were acquired through a UPS system (AXIS nova, Kratos Analytical), equipped with a helium ultraviolet source of 21.22 eV. The absorbance spectra were measured with a UV-Vis spectrophotometer (Ultrospec 2100 pro, Biochrom). EPR spectra were acquired using an electron spin resonance spectrometer (JEOL, JES-X320). *I-V* curves were measured by incrementally raising the DC voltage by 10 mV steps from −2V to +2V, measuring the corresponding currents. PLQY was obtained using a UV-NIR absolute PL quantum yield spectrometer (Hamamatsu, C13534) with a high-power Xe lamp. IR camera images were obtained using PI640 microscope optics.

Device Fabrication

−□.□□□ eV (TzTPT-INCN) and −□.□□□ eV, respectively (TzCDT-INCN).

The ITO-coated substrate (1.5 × 1.5 cm²) was subjected to a cleaning process using ultrasonication with acetone, isopropyl alcohol, and deionized water for 15 minutes each. Subsequently, a 30-minute UV ozone treatment was applied. The ITO was then spin-coated with a 3 mmol MeO-4PACz ethanol solution at 5000 rpm for 30 seconds and heated at 100 °C for 10 minutes. Ethanol rinse at 5000 rpm for 30 seconds followed to remove unattached molecules. Next, a 1.4 M solution of $FA_{0.85}Cs_{0.15}PbI_3$ in DMF/DMSO (7:3 v/v) was spin-coated onto the MeO-4PACz layer at 500 rpm for 8 seconds, followed by 3000 rpm for 25 seconds. The ethyl acetate (450 μL) was dropped onto the substrate 10 seconds before spinning ended. The resulting perovskite layer was annealed at 100 °C for 50 minutes. Subsequently, the (n-doped) $PC_{61}B$-TEG solution was spin-coated on the perovskite layer at 5000 rpm for 30 seconds and annealed at 100 °C for 10 minutes. A 30 nm-thick C_{60} layer was thermally evaporated under high vacuum (< 5×10^{-5} torr) at an evaporation rate of 0.5 Å. A 100 nm thick Ag electrode was evaporated through a shadow mask, defining the active area to 0.135 cm². Additionally, LiF (70 nm thick) was evaporated on the glass side to mitigate reflection loss from the glass substrate.

Supplementary note 1

Thermal conductivity measurement

Thermal conductivity (κ) measurements were conducted using a time-domain thermoreflectance (TDTR) technique. A detailed description of the measurement principle and experimental setup can be found elsewhere.[3-4] A femtosecond pulsed laser, generated by a Ti:Sapphire oscillator with an 80 MHz repetition rate, was split into pump and probe beams using a half-wave plate and a polarized beam splitter (PBS). The pump beam passed through an electro-optic modulator (EOM) with sinusoidal modulation, followed by frequency doubling through a bismuth borate (BIBO) crystal. The probe beam, delayed by a mechanical stage ranging from 0 to 5000 ps, was coaxially excited with the pump beam at the sample surface. Reflectance changes induced by the pump beam were measured using the probe beam. A thin layer of aluminum film (80 nm) deposited on the top layer of the sample served as an opto-thermal transducer. The thermal conductivity (κ) of the sample was determined by fitting experimental data to thermal modeling.

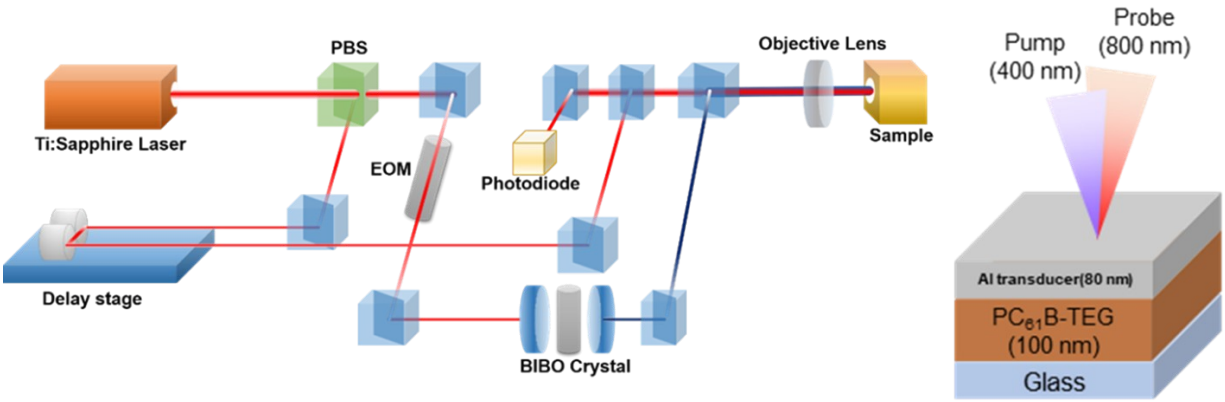

Schematics of TDTR measurement and sample structure.

Heat capacity measurement

The volumetric heat capacity (C_v) of the $PC_{61}B$-TEG samples was estimated by multiplying the specific heat capacity (C_p) by the density of $PC_{61}B$-TEG (ρ). The C_p value was obtained from differential scanning calorimetry (DSC) using Q200 (TA Instrument) (see Fig. S5, ESI†), while ρ was approximated to the density of [6,6]-phenyl C_{61} butyric acid methyl ester (PCBM) at 1.5 g/cm³. The C_p was measured using a step scan isothermal method from 20 to 30 ℃ with a scan rate of 0.1 ℃/minute and a 10-minute hold at every interval.

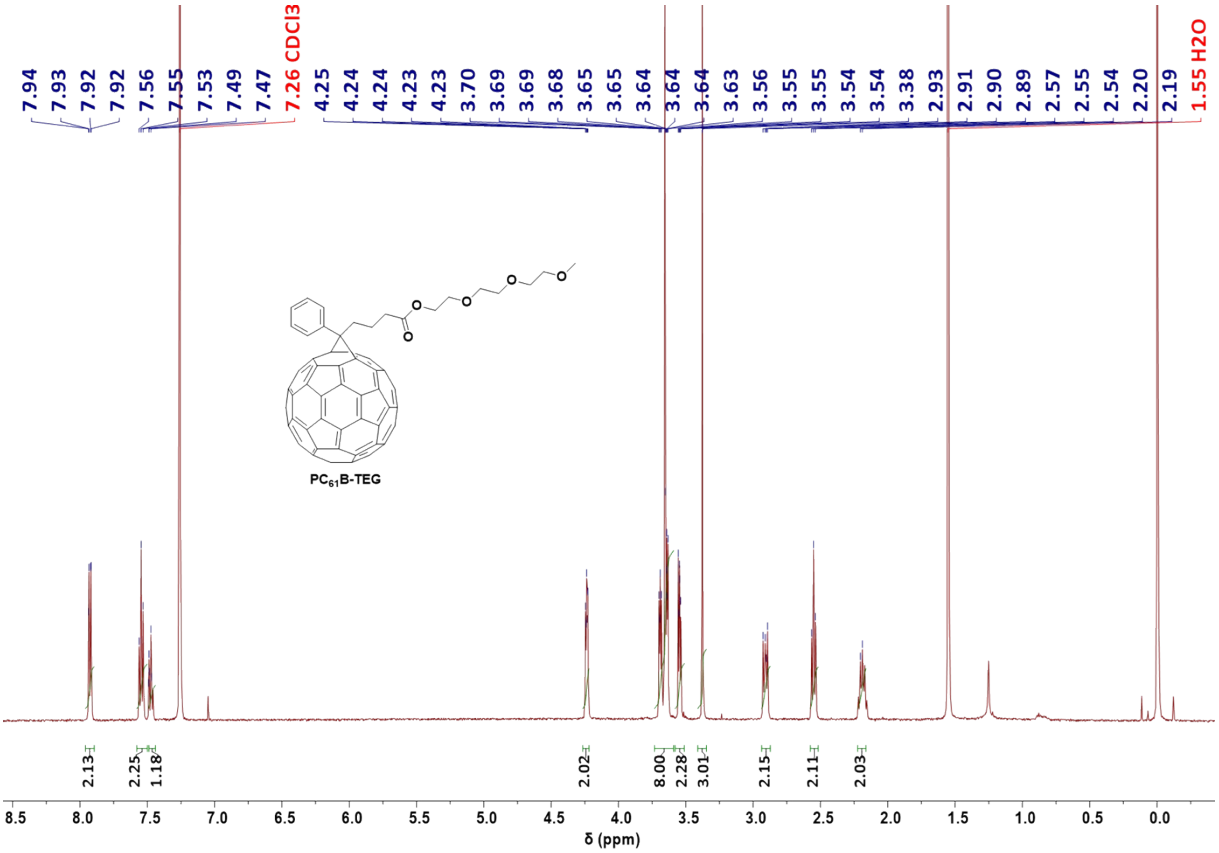

Fig. S1 ^{1}H-NMR spectrum of $PC_{61}B$-TEG in $CDCl_3$.

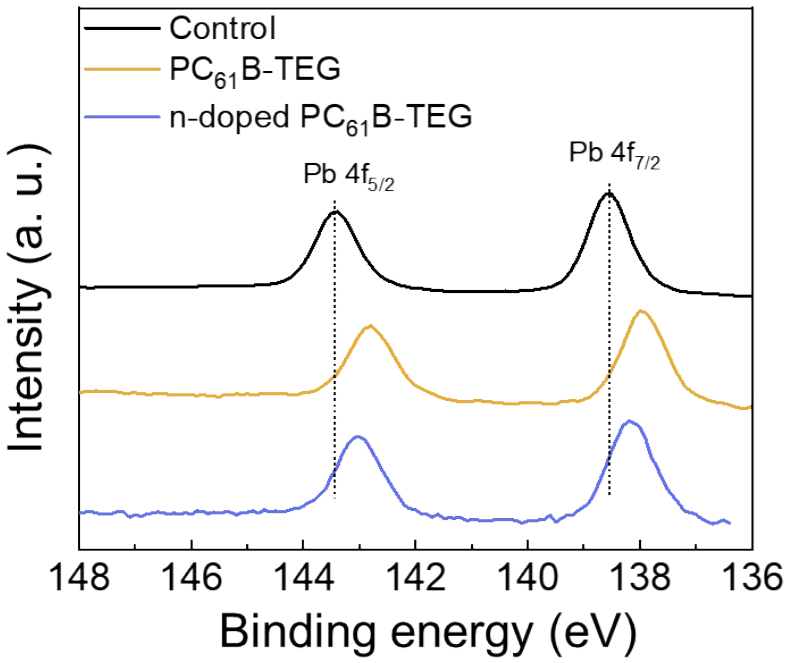

Fig. S2 Pb 4f XPS spectra of perovskite films with and without $PC_{61}B$-TEG and n-doped $PC_{61}B$-TEG.

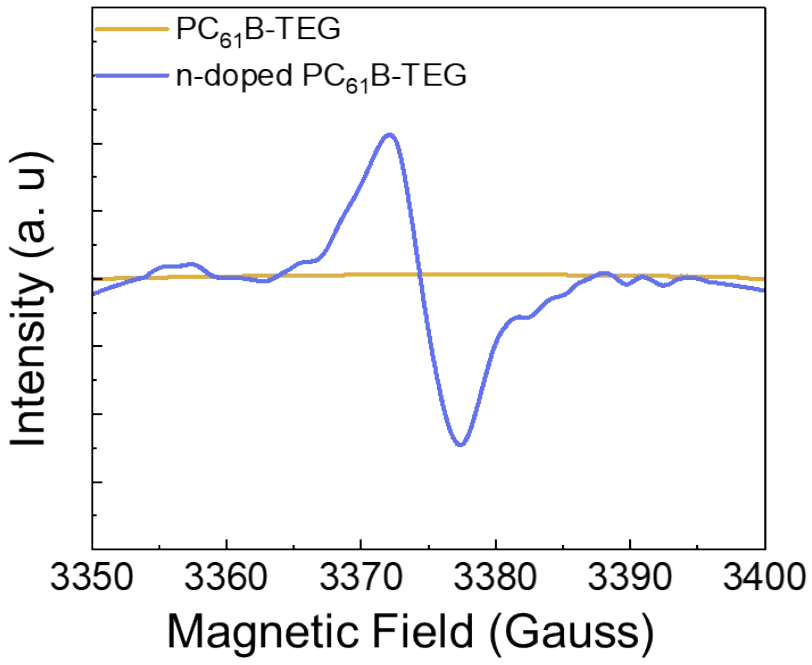

Fig. S3 EPR signal of $PC_{61}B$-TEG doped with N-DMBI as dopant.

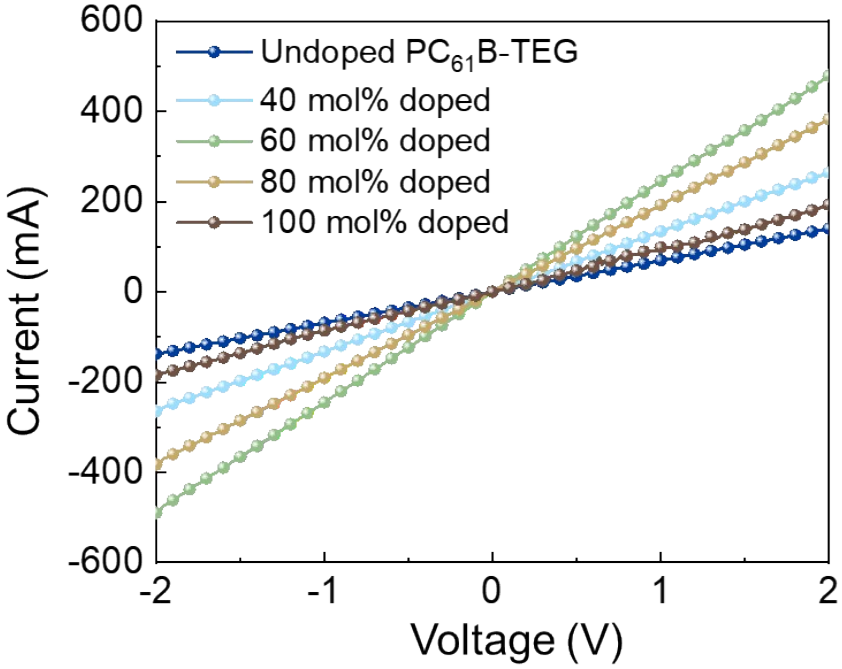

Fig. S4 Electrical conductivity of $PC_{61}B$-TEG films depending on doping concentration.

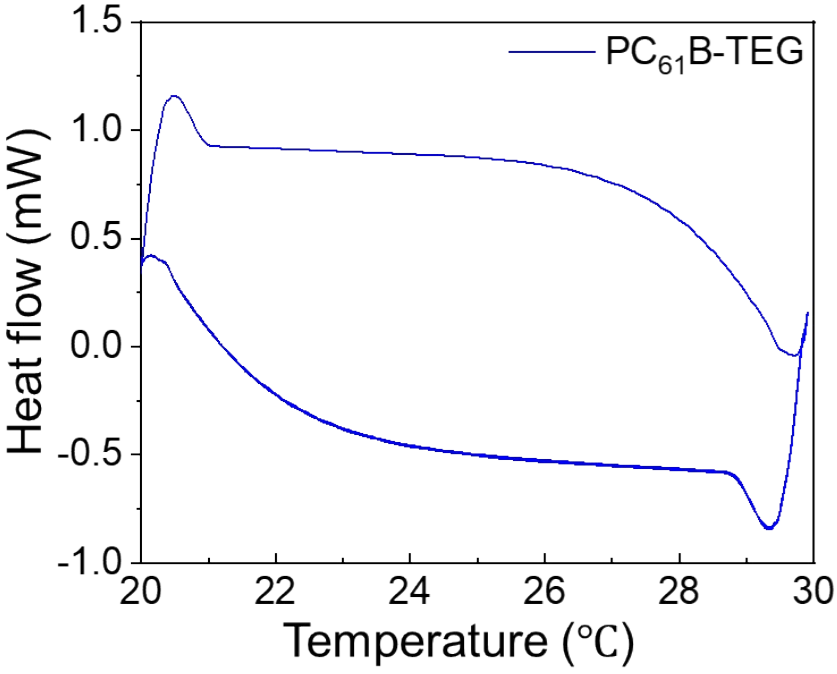

Fig. S5 DSC thermogram of $PC_{61}B$-TEG.

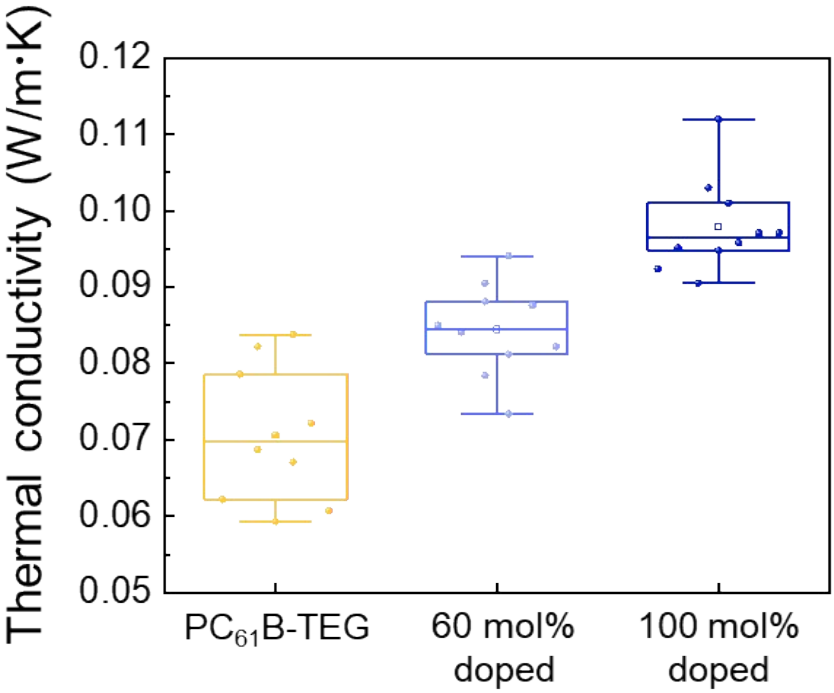

Fig. S6 Thermal conductivity statistics of undoped $PC_{61}B$-TEG and $PC_{61}B$-TEG doped with N-DMBI (60 and 100 mol%).

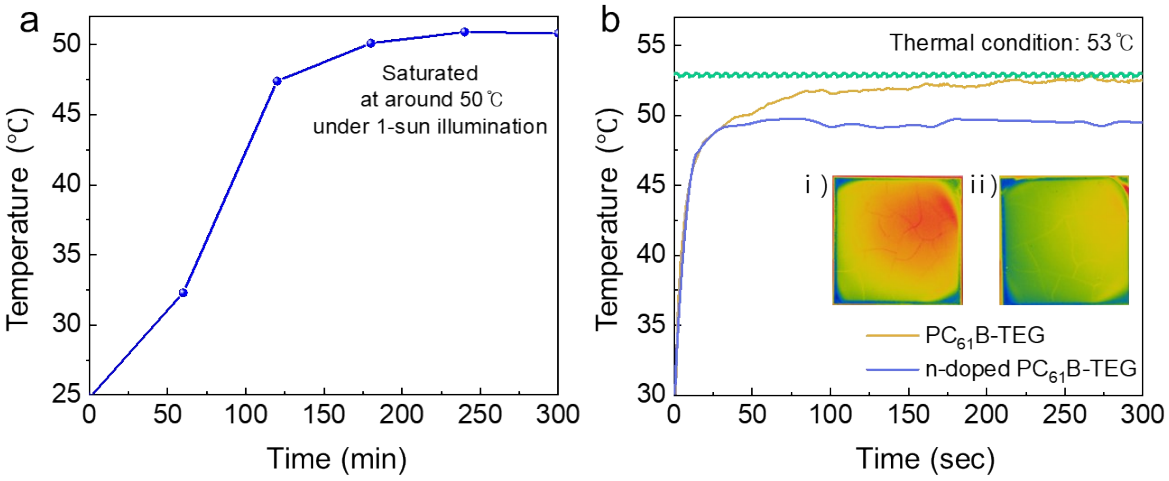

Fig. S7 (a) Temperature increment under 1-sun illumination condition of AM 1.5 G (100 mW cm^{-2}) (b) Temperature profiles of perovskite/$PC_{61}B$-TEG film with and without n-doping under 53 ℃ continuous heat. Insets are IR camera images of perovskite/$PC_{61}B$-TEG films of i) without and ii) with n-doping heated continuously for 5 minutes at 53 ℃.

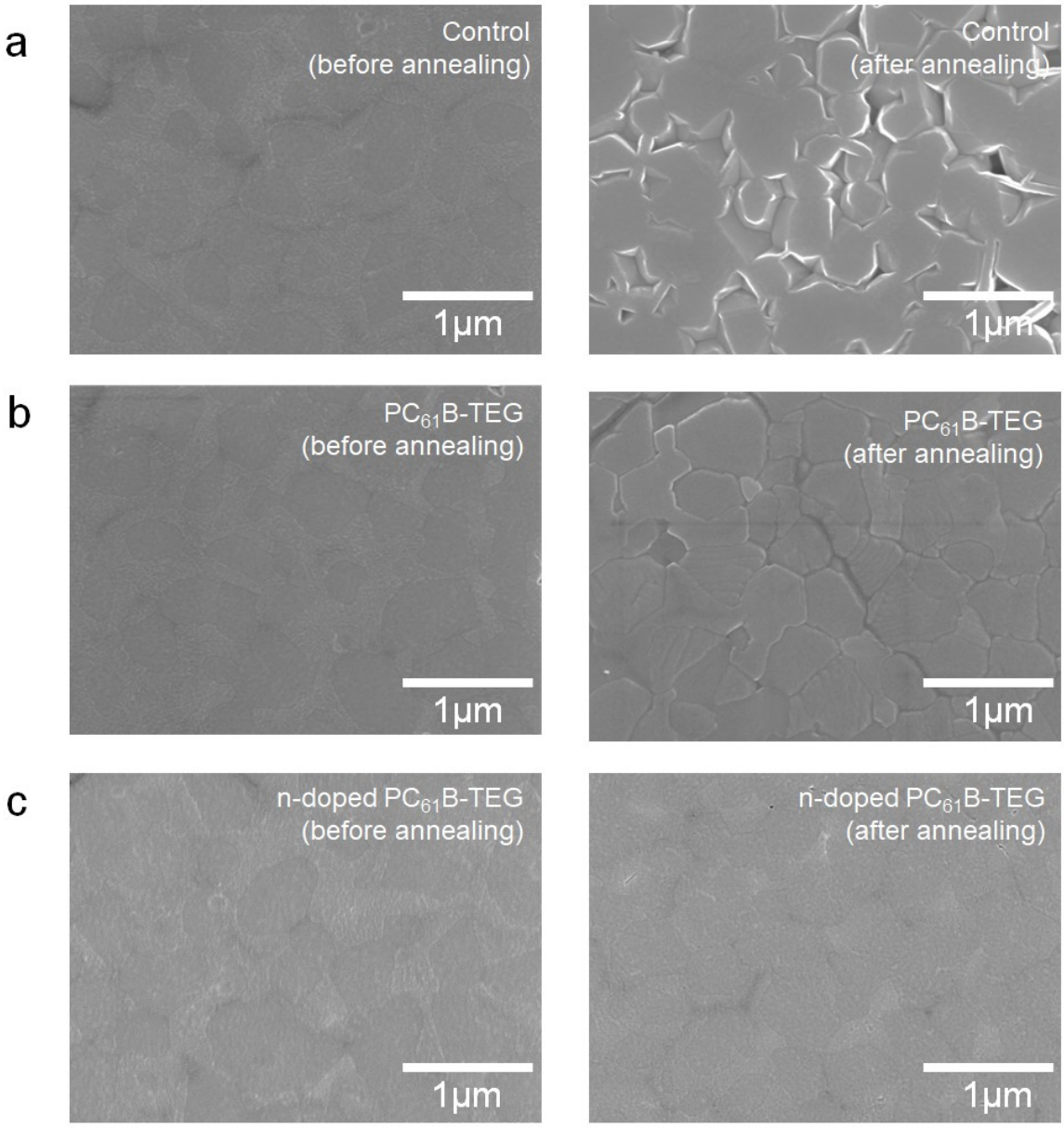

Fig. S8 SEM images of the bottom side perovskite films (a) without (control) and (b) with $PC_{61}B$-TEG, and (C) n-doped $PC_{61}B$-TEG. The "after annealing" samples were heated at 120 ℃ for 72 hours in N_2.

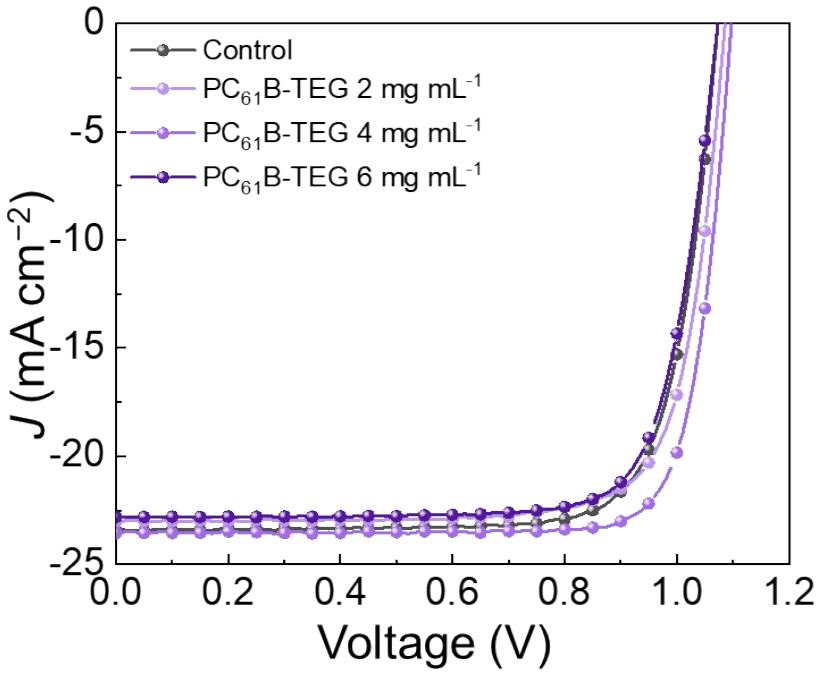

Fig. S9 *J-V* curve of PeSCs with a $PC_{61}B$-TEG top interlayer with variation of its concentration.

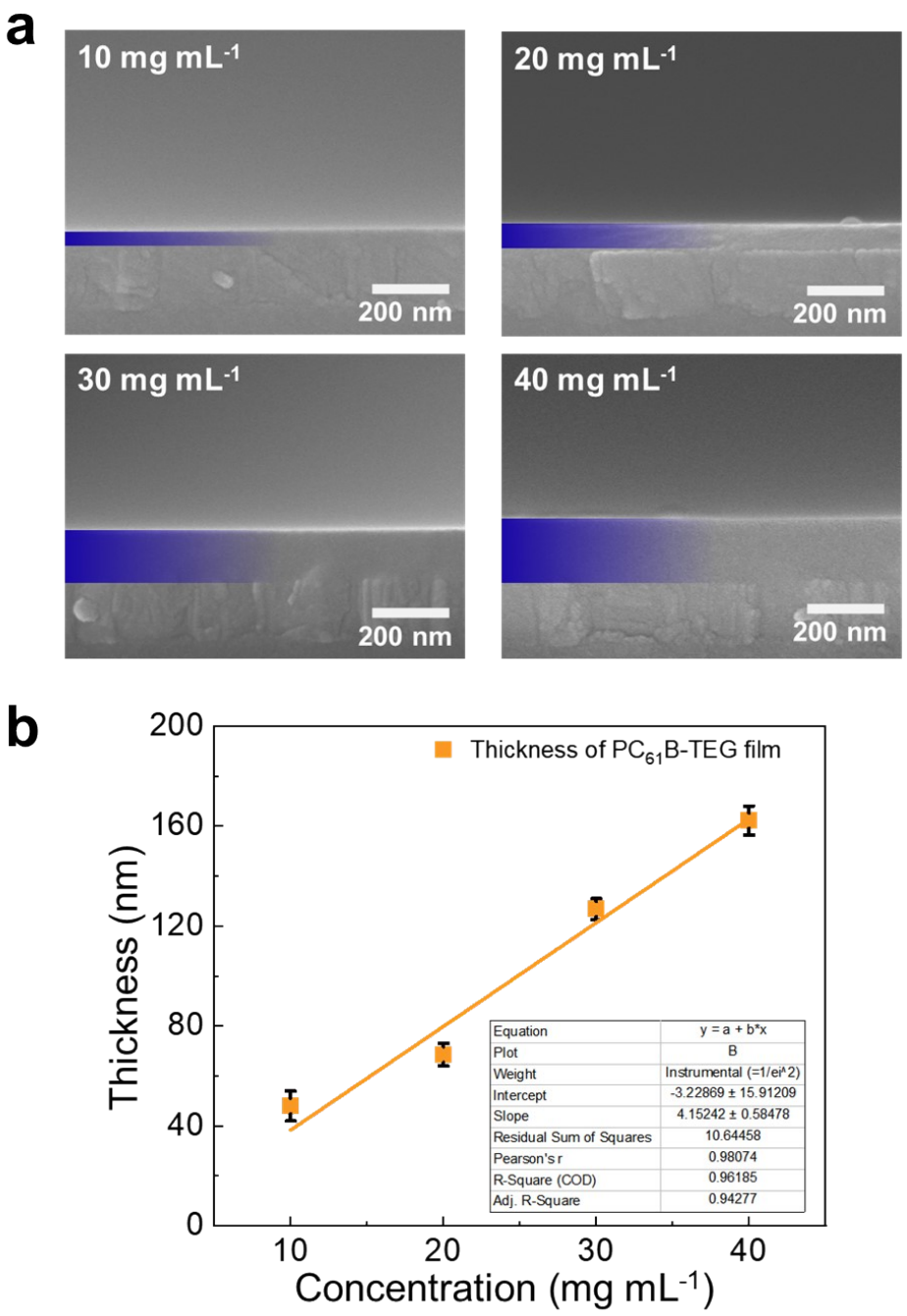

Fig. S10 Thickness confimation of $PC_{61}B$-TEG (a) SEM images of cross-sections $PC_{61}B$-TEG depend on various concentration**.** $PC_{61}B$-TEG films are fabricated by spin coating $PC_{61}B$-TEG solutions (dissolved in chloroform) in 5000 rpm for 30 sec on ITO substrates. (b) Correlation between the concentration of $PC_{61}B$-TEG solution and thickness of $PC_{61}B$-TEG film.

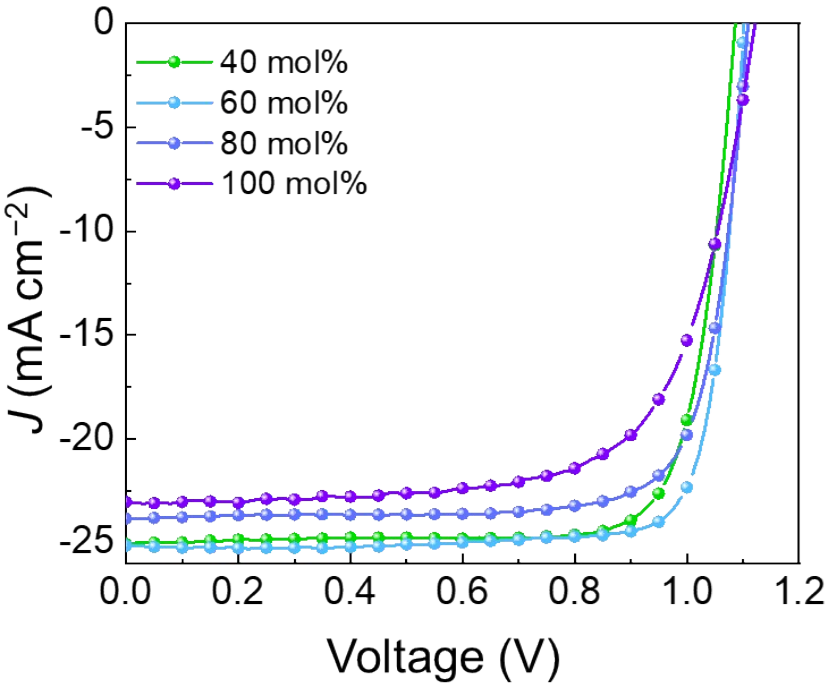

Fig. S11 *J-V* curve of PeSCs with n-doped $PC_{61}B$-TEG interlayer by varying doping concentration.

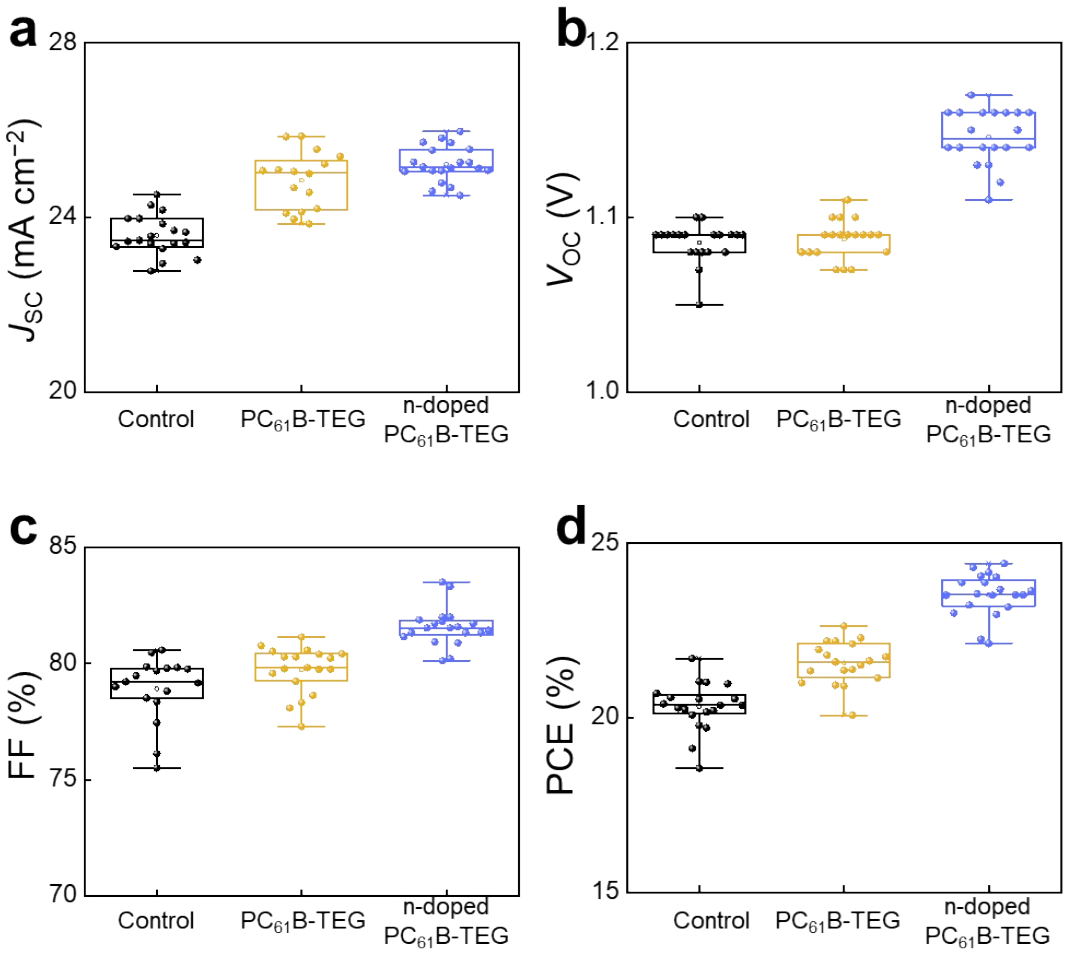

Fig. S12 Statistics og photovoltaic parameters of PeSCs (a) J_{SC}, (b) V_{OC} (c) FF and (d) PCE of control, PC$_{61}$B-TEG and n-doped PC$_{61}$B-TEG .

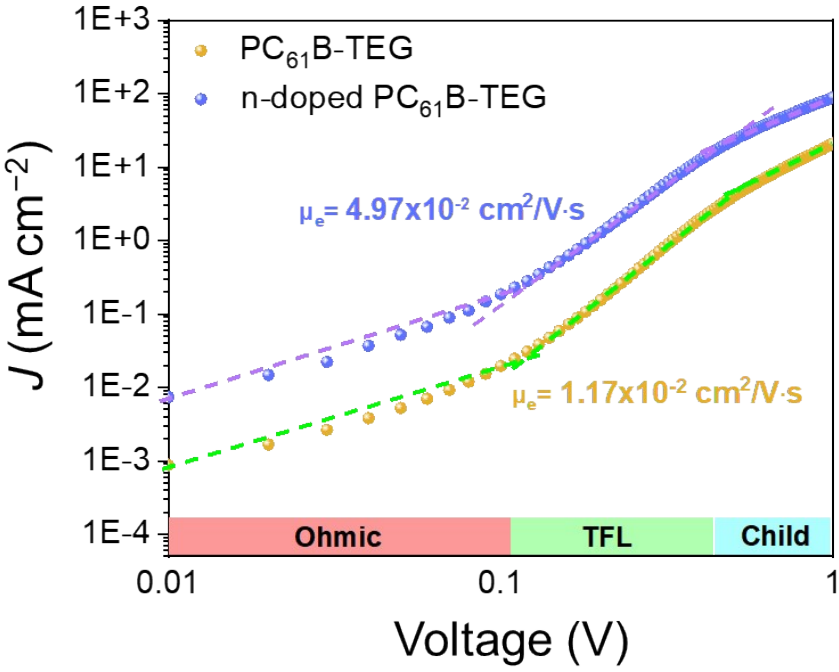

Fig. S13 SCLC curves of electron-only devices with an architecture of ITO/SnO_2/(n-doped) $PC_{61}B$-TEG/LiF/Ag.

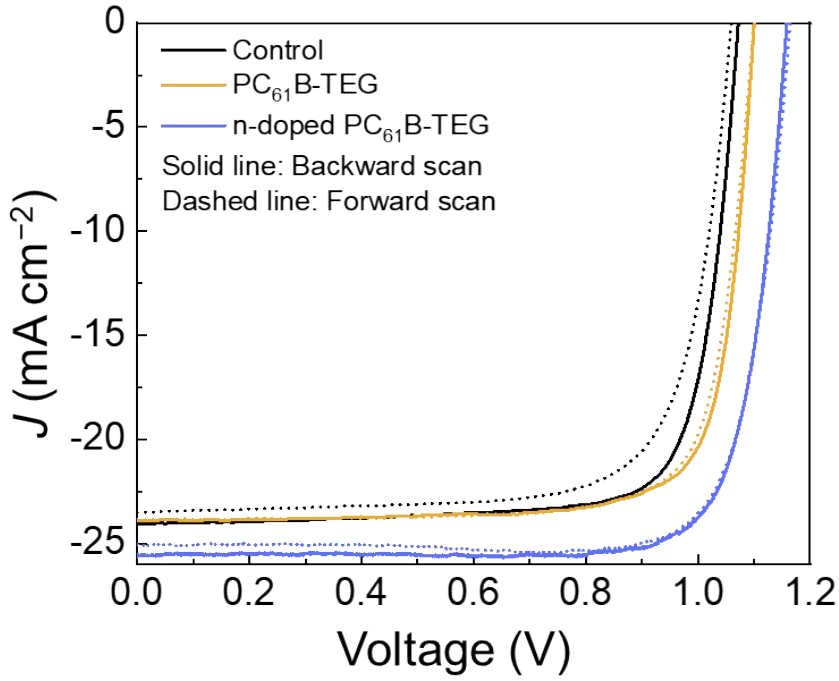

Fig. S14 *J-V* curves of Control, $PC_{61}B$-TEG and n-doped $PC_{61}B$-TEG treated PeSCs under forward and backward scans.

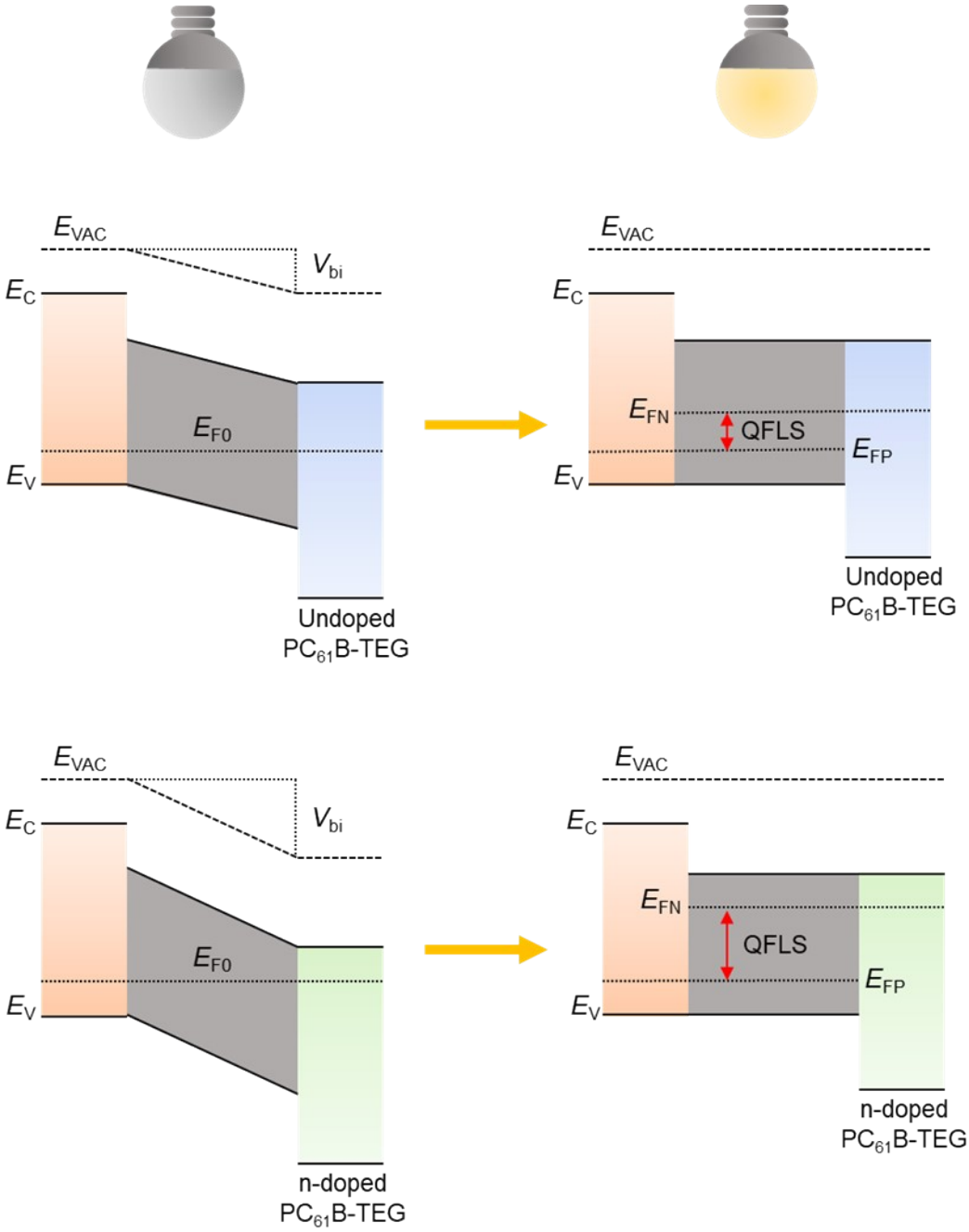

Fig. S15 Illustrations of QFLS in PeSCs with undoped $PC_{61}B$-TEG and n-doped $PC_{61}B$-TEG interlayers.

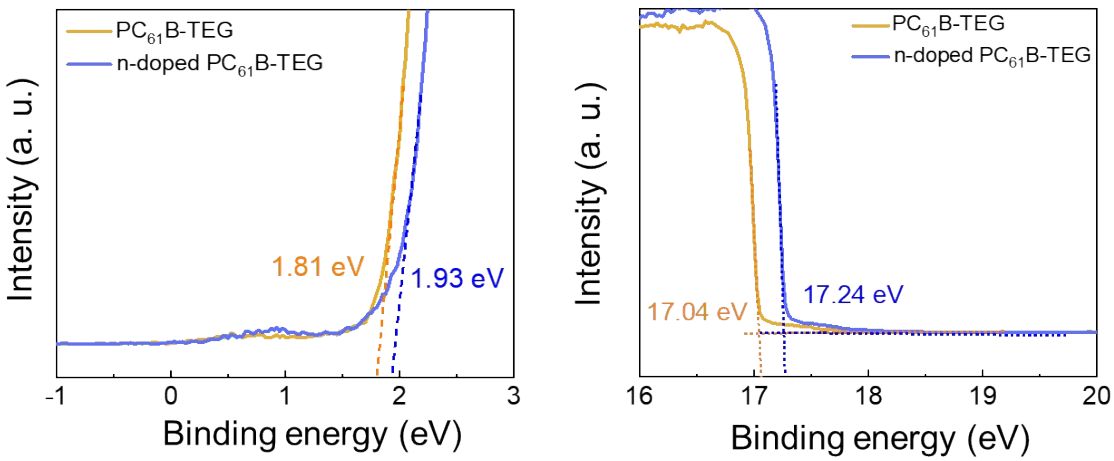

Fig. S16 UPS measurement of $PC_{61}B$-TEG and n-doped $PC_{61}B$-TEG in optimized doping concentration.

Table S1 Resistance and electrical conductivity of $PC_{61}B$-TEG and n-doped $PC_{61}B$-TEG films (40, 60, 80, 100 mol%).

Doping concentration	Resistance [Ω]	Conductivity [S cm^{-1}]
$PC_{61}B$-TEG	14.27	4.41×10^{-4}
40 mol%	7.54	1.19×10^{-3}
60 mol%	4.13	2.17×10^{-3}
80 mol%	5.24	1.17×10^{-3}
100 mol%	10.87	8.24×10^{-4}

Table S2 XRD peak area ratios of PbI_2/(100) for control, $PC_{61}B$-TEG, and n-doped $PC_{61}B$-TEG treated cells before and after thermal treatment at 120 ℃ for 72 hours.

	PbI_2/(100) before treatment	PbI_2/(100) after treatment
Control	0.186	3.128
$PC_{61}B$-TEG	0.166	1.492
n-doped $PC_{61}B$-TEG	0.101	0.197

Table S3 Photovoltaic parameters of PeSCs with undoped $PC_{61}B$-TEG interlayer.

Concentration of $PC_{61}B$-TEG	J_{SC} [mA cm^{-2}]	V_{OC} [V]	FF [%]	PCE [%]
Control	23.43	1.07	76.93	19.47
2 mg mL^{-1}	23.04	1.09	77.53	19.47
4 mg mL^{-1}	23.67	1.1	81.45	21.11
6 mg mL^{-1}	22.81	1.08	77.44	19.08

Table S4 Photovoltaic parameters of PeSCs with undoped $PC_{61}B$-TEG interlayer.

Doping concentration	J_{SC} [mA cm^{-2}]	V_{OC} [V]	FF [%]	PCE [%]
40 mol%	25.05	1.09	79.24	21.64
60 mol%	25.13	1.11	81.82	22.83
80 mol%	22.71	1.12	71.58	18.21
100 mol%	23.02	1.13	68.53	17.83

Table S5 Photovoltaic parameters of control and (n-doped) $PC_{61}B$-TEG treated PeSCs under backward and forward scans.

Device	Scan direction	V_{OC} [V]	J_{SC} [mA cm^{-2}]	FF [%]	PCE [%]	HI[a)] [%]
Control	Backward	1.08	24.05	77.78	20.21	8.21
	Forward	1.05	23.51	75.10	18.55	
$PC_{61}B$-TEG	Backward	1.11	23.88	78.79	20.89	1.15
	Forward	1.09	23.84	79.48	20.65	
n-doped $PC_{61}B$-TEG	Backward	1.16	25.60	80.36	23.85	0.88
	Forward	1.16	25.05	80.99	23.64	

a) Hysteresis index.

References

1. K. Kim, Z. Wu, J. Han, Y. Ma, S. Lee, S.-K. Jung, J.-W. Lee, H. Y. Woo and I. Jeon, *Adv. Energy Mater.*, 2022, **12**, 2200877
2. M. P. Hughes, K. D. Rosenthal, R. R. Dasari, B. R. Luginbuhl, B. Yurash, S. R. Marder and T.-Q. Nguyen, *Adv. Func. Mater.*, 2019, **29**, 1901269.
3. D. G. Cahill, *Rev. Sci. Instrum.*, 2004, **75**, 5119.
4. A. J. Schmidt, X. Chen and G. Chen, *Rev. Sci. Instrum.*, 2008, **79**, 114902.